symmetry

MDPI

Article

Constraints on the String T-Duality Propagator from the Hydrogen Atom

Michael F. Wondrak [1,2,*] and Marcus Bleicher [1,2]

[1] Frankfurt Institute for Advanced Studies (FIAS), Ruth-Moufang-Straße 1, 60438 Frankfurt am Main, Germany
[2] Institut für Theoretische Physik, Johann Wolfgang Goethe-Universität Frankfurt am Main, Max-von-Laue-Straße 1, 60438 Frankfurt am Main, Germany; bleicher@th.physik.uni-frankfurt.de
* Correspondence: wondrak@fias.uni-frankfurt.de

Received: 17 October 2019; Accepted: 29 November 2019; Published: 4 December 2019

Abstract: We investigated the implications of string theory in the high-precision regime of quantum mechanics. In particular, we examined a quantum field theoretical propagator which was derived from string theory when compactified at the T-duality self-dual radius and which is closely related to the path integral duality. Our focus was on the hydrogen ground state energy and the $1S_{1/2} - 2S_{1/2}$ transition frequency, as they are the most precisely explored properties of the hydrogen atom. The T-duality propagator alters the photon field dynamics leading to a modified Coulomb potential. Thus, our study is complementary to investigations where the electron evolution is modified, as in studies of a minimal length in the context of the generalized uncertainty principle. The first manifestation of the T-duality propagator arises at fourth order in the fine-structure constant, including a logarithmic term. For the first time, constraints on the underlying parameter, the zero-point length, are presented. They reach down to 3.9×10^{-19} m and are in full agreement with previous studies on black holes.

Keywords: string T-duality; zero-point length; minimal length; extra dimensions; modified Coulomb potential; hydrogen energy levels

1. Introduction

Symmetries lie at the heart of almost any theory in physics and imply far-reaching consequences: symmetries powerfully constrain the structure of terms that are allowed in a given action; e.g., of the electroweak theory [1]. They allow one to clearly extract the fundamental degrees of freedom of a theory by choosing an appropriate gauge (cf. gravitational waves; e.g., [2,3]). In the context of string theory, there are even symmetries which show the equivalence of whole theories. Among those is T-duality, which acts on the moduli space and relates string theories compactified on different backgrounds.

As a special case, T-duality relates toroidally compactified theories which emerge from each other under inversion of the compactification radius, R, and exchange of the Kaluza-Klein mode numbers, n, with the winding mode numbers, w. In the case of one extra dimension, the relation reads $R \to R^{\star 2}/R$ and $n \leftrightarrow w$. The self-dual radius $R^\star$ is mapped onto itself while compactification radii smaller than $R^\star$ are identified with larger ones. Thus, a notion of a smallest sensible length scale arises. The self-dual radius is located at the string scale, $R^\star = \sqrt{\alpha'}$, where α' denotes the Regge slope.

Starting from toroidally compactified bosonic string theory with compactification radius $R^\star$, the authors of [4] derived an effective 4-dimensional propagator for the center-of-mass of closed strings (cf. also [5,6]). Compared to standard quantum field theory propagators, the presence of compactified extra dimensions implies a UV finite behavior. There are contributions from a tower of momentum and winding modes, out of which the massless mode is the most relevant for low-energy

physics. It gives rise to the T-duality propagator. The T-duality propagator found its first, and so far, only application in the recent derivation of a quantum-gravity corrected black hole description [7]. Here, the self-dual radius plays a crucial role: It leads to a resolution of the curvature singularity at the black hole center and to a non-divergent black hole evaporation process without a final explosion. The latter difference to the Schwarzschild black hole solution offers an observable to test the hypothesis of the T-duality propagator.

A concept related to the T-duality ansatz which also tries to capture effects of the quantum nature of spacetime is the path integral duality. While the former is derived from string theory, the latter is an ad hoc ansatz in quantum field theory which introduces scale-inversion symmetric weights in the Schwinger representation of the propagator—at a scale known as zero-point length, l_0 [8,9]. Both the propagators, from the first order T-duality approach and from the path integral duality, agree. This allows one to relate the zero-point length to the self-dual radius, $l_0 = 2\pi R^\star = 2\pi\sqrt{\alpha'}$. Using effective actions, several quantum field theoretical aspects of the path integral duality have been examined; e.g., the Casimir effect and the thermal particle spectra of Rindler vacua [10]. In the context of gravity, investigations in the curved spacetime of cosmology [11,12] and of black holes [13] have been conducted. Recently, the regularization of path integrals has been generalized to the concept of so-called path densities [14]. But there are, to our knowledge, no studies that derive bounds on the zero-point length from experimental data.

For our work, modifications of electromagnetic interactions are relevant. In the literature, the path integral duality has been used to calculate deviations in the radiative corrections in quantum electrodynamics [15]. Radiative corrections for a whole family of propagators, which share a similar analytical structure and are referred to as smeared propagators, have been addressed earlier [16–18]. The aim of the present study is to analyze the concept of the T-duality induced zero-point length from a different, low-energy perspective. We chose a system in quantum physics which has been investigated to high precision theoretically and experimentally—the hydrogen atom [19]—and derive constraints on l_0. The hydrogen atom has been used by several authors to test various high-energy concepts; e.g., [20–24].

We used two characteristics of the hydrogen atom: firstly, the ground state energy, and secondly, the transition frequency between the two lowest energy levels with vanishing orbital angular momentum, $1S_{1/2}$ and $2S_{1/2}$—the spectral line which is experimentally known to highest precision [25]. The potential shift in these observables due to the T-duality concept strongly depends on the size of l_0. We calculated those in Rayleigh–Schrödinger perturbation theory. From comparison with discrepancies between experimental and theoretical values and from their uncertainties, we obtained upper limits of l_0.

In Section 2, we review the theoretical description of the hydrogen atom. We obtain the energy and frequency corrections from the T-duality propagator. The constraints from both observables are derived in Section 3 and are discussed in Section 4. Section 5 offers a summary. Useful mathematical identities are presented in the Appendix A. In this article we use natural units; in particular, $c \equiv \hbar \equiv 1$. For electromagnetic quantities we apply the Lorentz–Heaviside convention which additionally implies $\epsilon_0 \equiv \mu_0 \equiv 1$.

2. Hydrogen Atom Energy Levels

The hydrogen atom is a prime object in quantum mechanics. This section focuses on the energy spectrum in the conventional description and on the corrections arising from a T-self-dual spacetime. We start with the Schrödinger equation with fine-structure terms because we are considering a low-energy quantum system. Then, we introduce the T-duality induced modifications of the Coulomb potential. Finally, we derive shifts in energy levels and transition frequencies.

2.1. Conventional Description

The stationary Schrödinger equation, $H_0 \left|\psi\right\rangle = E \left|\psi\right\rangle$, with the eigenvectors $\left|\psi\right\rangle$ and eigenvalues E, is the starting point of our recapitulation which follows the references [26,27]. In position space, the Hamiltonian for spherically symmetric systems is given by

$$H_0 = -\frac{1}{2\mu}\,\Delta + V_0 = -\frac{1}{2\mu r^2}\,\partial_r\left(r^2\partial_r\right) + \frac{\vec{L}^2}{2\mu r^2} + V_0. \tag{1}$$

Here, μ is the reduced mass of the electron-proton system, Δ is the Laplace operator, and $\vec{L}$ the angular momentum operator. The potential term follows directly from the Coulomb interaction,

$$V_0 = -\frac{\alpha}{r}, \tag{2}$$

where $\alpha = e^2/4\pi$ denotes Sommerfeld's fine-structure constant. The well-known separation ansatz in spherical coordinates reads

$$\psi^{(0)}_{nlm}(r,\vartheta,\varphi) \equiv \left\langle \vec{r} \;\middle|\; nlm^{(0)} \right\rangle = \frac{u_{nl}\,(r)}{r}\,Y_{lm}(\vartheta,\varphi)\,, \tag{3}$$

with the principle, the orbital angular momentum, and the magnetic quantum numbers n, l, and m. The spherical harmonics $Y_{lm}(\vartheta,\varphi)$ solve the angular part while the radial equation simplifies to

$$\left(-\frac{1}{2\mu}\,\frac{d^2}{dr^2} + \frac{1}{2\mu}\,\frac{l\,(l+1)}{r^2} - \frac{\alpha}{r}\right) u_{nl}(r) = E_n\,u_{nl}(r)\,, \tag{4}$$

with the bound-state solutions

$$u_{nl}(r) = -\left[\frac{(n-l-1)!\,(2\kappa)^3}{2n\left((n+l)!\right)^3}\right]^{1/2} r\,(2\kappa r)^l\,\mathrm{e}^{-\kappa r}\,L^{2l+1}_{n+l}\,(2\kappa r)\,. \tag{5}$$

Herein, we define $\kappa \equiv \mu\alpha/n$ and apply the associated Laguerre polynomials

$$L^s_r\,(x) = \sum_{k=0}^{r-s}(-1)^{k+s}\,\frac{(r!)^2}{k!\,(k+s)!\,(r-k-s)!}\,x^k. \tag{6}$$

The spectrum of the energy eigenstates is discrete and depends on n only,

$$E_n = -\frac{\mu\alpha^2}{2}\,\frac{1}{n^2}. \tag{7}$$

The ground state, denoted by $1S_{1/2}$, shows the energy $E^{\mathrm{S}}_{\mathrm{th}} \equiv E_1 = -\mu\alpha^2/2$. Below, we will also employ the first excited state of spherical symmetry, $2S_{1/2}$. The associated wave functions read

$$\psi^{(0)}_{100} = \frac{2}{\sqrt{4\pi}}\,(\mu\alpha)^{3/2}\,e^{-\alpha\mu r} \tag{8}$$

$$\psi^{(0)}_{200} = \frac{2}{\sqrt{4\pi}}\left(\frac{\mu\alpha}{2}\right)^{3/2}\left[1-\frac{1}{2}\,\alpha\mu r\right]\,e^{-\alpha\mu r/2}, \tag{9}$$

and the transition frequency between both states follows to be $\nu^{\mathrm{S}}_{\mathrm{th}} \equiv (E_2 - E_1)\,/2\pi$.

Next, we include relativistic corrections which lead to the so-called fine structure in the spectrum. These are encoded in the relativistically adjusted Hamiltonian $H = H_0 + H_{\mathrm{fs}}$. The terms for

relativistic momentum correction, spin-orbit coupling, and zitterbewegung (Darwin term) constitute the Hamiltonian contribution

$$H_{\rm fs} = -\frac{\Delta^2}{8\mu^3} + \frac{\alpha}{4\mu^2 r^3}\,\vec{\sigma}\cdot\vec{L} + \frac{1}{8\mu^2}\,(\Delta V_0)\,, \tag{10}$$

which involves the Pauli matrices, $\vec{\sigma}$.

The correction in the energy spectrum can be calculated by means of the time-independent Rayleigh–Schrödinger perturbation theory. The first order corrections partially break the degeneracy and explicitly depend on the total angular momentum quantum number $j = l + s = l \pm 1/2$. They read

$$\Delta E^{\rm fs}_{n,j} = \left\langle nlm^{(0)} \,\middle|\, H_{\rm fs} \,\middle|\, nlm^{(0)} \right\rangle \tag{11}$$

$$= \frac{\mu\alpha^2}{2n^2}\,\frac{\alpha^2}{n^2}\left(\frac{3}{4} - \frac{n}{j+1/2}\right). \tag{12}$$

In particular, the corrections to the $1S_{1/2}$ and $2S_{1/2}$ levels are

$$\Delta E^{\rm fs}_{1,1/2} = -\frac{\mu\alpha^2}{2}\,\frac{\alpha^2}{4}, \qquad \Delta E^{\rm fs}_{2,1/2} = -\frac{\mu\alpha^2}{2}\,\frac{5\alpha^2}{128}. \tag{13}$$

We define the improved value of the ground state energy as $E^{\rm fs}_{\rm th} \equiv E_1 + \Delta E^{\rm fs}_{1,1/2}$ and the corrected transition frequency as $\nu^{\rm fs}_{\rm th} \equiv \left(\left(E_2 + \Delta E^{\rm fs}_{2,1/2}\right) - \left(E_1 + \Delta E^{\rm fs}_{1,1/2}\right)\right)/2\pi$.

The fine-structure corrections naturally arise in the Dirac treatment of the hydrogen atom and agree with Equation (12) to order α^4. The state-of-the-art description of the hydrogen atom goes beyond idealizations like that of a point-like nucleus or vanishing nuclear polarizability, and uses methods of quantum field theory to include, e.g., multiple photon interactions in quantum electrodynamics or hadronic contributions to the proton self-energy from quantum chromodynamics. Those corrections appear at order α^5 or higher. For an overview of the contributions, we refer the reader to [19].

2.2. Contribution from T-Duality Propagator

The considerations up to now originate from quantum mechanics and quantum field theory. The standard model of particle physics, however, is generally being assumed to be incomplete. In contrast, superstring theory is a possible candidate for a unified theory also valid at high energies which reduces to the standard model and to general relativity as limiting cases [28]. In the following we consider closed bosonic string theory on a manifold with toroidal compactification where the compactification radius equals the self-dual radius under T-duality. Regarding the 4-dimensional propagation, the string center of mass deviates from excitations of quantum fields. The Euclidean propagator of a massless scalar field inherited from bosonic string theory reads [7]

$$G(k) = -\frac{l_0}{\sqrt{k^2}}\,K_1\left(l_0\sqrt{k^2}\right) \to \begin{cases} -1/k^2 & \text{if } k^2 \ll 1/{l_0}^2 \\ -{l_0}^{1/2}\left(k^2\right)^{-3/4} e^{-l_0\sqrt{k^2}} & \text{if } k^2 \gg 1/{l_0}^2 \end{cases}, \tag{14}$$

where $K_\nu(x)$ are modified Bessel functions of the second kind. In the low-momentum limit, one obtains the standard scalar propagator, while there is an exponential suppression for momenta large compared to $1/l_0$.

We regard such a kinetic modification to apply to all quantum fields, especially to bosons. Virtual-particle exchange then leads to modified interaction potentials which contain the zero-point length as a UV cutoff [7]. In electrodynamics, the potential energy reads

$$V_{\rm Td} = -\frac{\alpha}{\sqrt{r^2 + {l_0}^2}}. \tag{15}$$

The difference to the conventional Coulomb interaction can be used to identify manifestations of T-duality from the hydrogen energy spectrum. From that we can derive constraints on l_0. Similar to the inclusion of fine-structure corrections, we apply the Rayleigh–Schrödinger perturbation theory to the amended Hamiltonian $H = H_0 + H_{\mathrm{fs}} + H_{\mathrm{Td}}$. The additional term comprises the modification of the Coulomb energy,

$$H_{\mathrm{Td}} = V_{\mathrm{Td}} - V_0 = \frac{\alpha}{r} - \frac{\alpha}{\sqrt{r^2 + {l_0}^2}}, \tag{16}$$

which is presented in Figure 1.

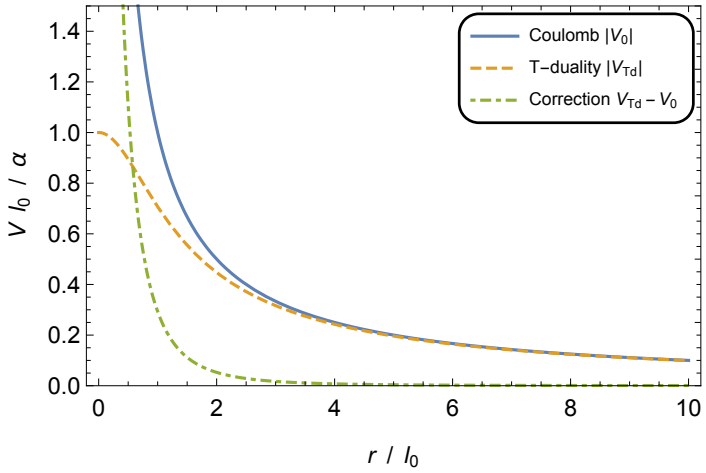

Figure 1. Potential energy. The solid curve (blue) displays the absolute value of the conventional Coulomb energy, $|V_0|$, while the dashed line (orange) shows the absolute value of the T-duality corrected energy, $|V_{\mathrm{Td}}|$. The difference of both equals the Hamiltonian contribution H_{Td} (dot-dashed curve, green).

In general, the level shifts depend on n and l,

$$\Delta E^{\mathrm{Td}}_{n,l} = \left\langle nlm^{(0)} \middle| H_{\mathrm{Td}} \middle| nlm^{(0)} \right\rangle \tag{17}$$

$$= \frac{2^{2+2l}\,(n-l-1)!\,\mu\alpha^2}{n^{4+2l}\left((n+l)!\right)^3} \times \int_0^\infty \mathrm{d}y\; y^{2+2l}\,\mathrm{e}^{-2y/n}\left[L^{2l+1}_{n+l}\,(2y/n)\right]^2 \left(\frac{1}{y} - \frac{1}{\sqrt{y^2+x^2}}\right). \tag{18}$$

Here we introduce $y \equiv \alpha\mu r$ and define $x \equiv \lambda_0\alpha$ where $\lambda_0 \equiv \mu l_0$. For the ground state, we find the following expression at first order in perturbation theory:

$$\Delta E^{\mathrm{Td}}_{1,0} = \frac{\mu\alpha^2}{2}\left(2 + \frac{16}{3}\,x^3 + 2\pi x\left[Y_1(2x) + \mathbf{H}_1(2x)\right] - 4\pi x^2\left[Y_0(2x) + \mathbf{H}_2(2x)\right]\right) \tag{19}$$

$$= \frac{\mu\alpha^2}{2}\left(\left[-2 - 4\gamma + 4\ln\frac{1}{x}\right]x^2 + \mathcal{O}\left(x^3\right)\right) \tag{20}$$

$$= \mu\lambda_0^2\left[-1 - 2\gamma + 2\ln\frac{1}{\alpha\lambda_0}\right]\alpha^4 + \mathcal{O}\left(\alpha^5\right). \tag{21}$$

We used the Euler–Mascheroni constant, $\gamma \approx 0.577$; the Bessel functions of the second kind, $Y_\nu(x)$; and the Struve functions, $\mathbf{H}_\nu(x)$. The level shift of $2S_{1/2}$ reads:

$$\begin{aligned}\Delta E^{\mathrm{Td}}_{2,0} &= \frac{\mu\alpha^2}{2}\left(\frac{1}{2}+\frac{3}{4}x^3+\frac{\pi}{4}\left(x+x^3\right)\left[Y_1(x)-\mathbf{H}_1(x)\right]\right. \\ &\quad \left.+\frac{\pi}{8}\left(-3x^2+x^4\right)\left[Y_0(x)-\mathbf{H}_0(x)\right]\right) \qquad (22)\\ &= \frac{\mu\alpha^2}{2}\left(\frac{1}{8}\left[-5-4\gamma+4\ln\frac{2}{x}\right]x^2+\mathcal{O}\left(x^3\right)\right) \qquad (23)\\ &= \frac{\mu\lambda_0^2}{16}\left[-5-4\gamma+4\ln\frac{2}{\alpha\lambda_0}\right]\alpha^4+\mathcal{O}\left(\alpha^5\right). \qquad (24)\end{aligned}$$

We provide the identities crucial in deriving this result in the Appendix A. Note that the corrections start at order α^4. Note also that they are of the form $\Delta E \propto \left(\text{const.}+\ln\frac{1}{\alpha\mu l_0}\right){l_0}^2$. For small values of l_0 the logarithmic term dominates ensuring the energy shifts to be positive. In contrast, the change in the transition frequency is negative for small values of l_0:

$$\begin{aligned}\Delta\nu^{\mathrm{Td}}_{1S-2S} &= \frac{1}{2\pi}\left(\Delta E^{\mathrm{Td}}_{2,0}-\Delta E^{\mathrm{Td}}_{1,0}\right) \qquad (25)\\ &= \frac{1}{2\pi}\frac{\mu\alpha^2}{2}\left(\frac{1}{8}\left[11+4\ln 2+28\gamma-28\ln\frac{1}{x}\right]x^2+\mathcal{O}\left(x^3\right)\right) \qquad (26)\\ &= \frac{\mu\lambda_0^2}{32\pi}\left[11+4\ln 2+28\gamma-28\ln\frac{1}{\alpha\lambda_0}\right]\alpha^4+\mathcal{O}\left(\alpha^5\right). \qquad (27)\end{aligned}$$

3. Constraints on the Zero-Point Length

In the previous section, we derived the shifts in the energy levels $1S_{1/2}$ and $2S_{1/2}$, and the shift in the associated transition frequency as a function of the zero-point length. Now we can contrast the shifts with experimental data in order to obtain constraints on the value of l_0.

3.1. Ground State Energy

The reference values and uncertainties of the hydrogen ground state energy from theory and experiment are displayed in Table 1. Taking into account the respective standard deviations, we take the maximum difference between the fine-structure improved Schrödinger value, $E^{\mathrm{fs}}_{\mathrm{th}}$, and the experimental one, E_{exp}, and that between the current theoretical value, $E^{\mathrm{QED}}_{\mathrm{th}}$, and the experimental one. In this context, the experimental precision ΔE_{exp} by itself defines the smallest upper bound on l_0.

Table 1. Theoretical and experimental values of the hydrogen ground state energy. The calculations of $E^{\mathrm{S}}_{\mathrm{th}}$ and $E^{\mathrm{fs}}_{\mathrm{th}}$ are based on the 2014 CODATA recommended values [19]. When expressed in eV, the actual precision of the current theoretical and experimental value is masked by the less-precisely known Planck constant [19]. For this reason, h is factored out and the values are given also in terms of MHz $\cdot$ h.

Energy	Description	Value
$E^{\mathrm{S}}_{\mathrm{th}}$	Schrödinger	−13.598 287 15(9) eV
$E^{\mathrm{fs}}_{\mathrm{th}}$	Schrödinger, incl. fine-structure	−13.598 468 18(9) eV
$E^{\mathrm{QED}}_{\mathrm{th}}$	current theoretical value [29]	−13.598 434 49(9) eV
		−3 288 086 857.1276(31) MHz · h
E_{exp}	current experimental value [25]	−13.598 434 48(9) eV
		−3 288 086 856.8(7) MHz · h

Figure 2 shows the relative T-duality contribution $\Delta E^{\mathrm{Td}}_{1,0}$ as a function of the zero-point length, l_0. The reference values are included as well. The zero-point length has to be smaller than the intersection point value to comply with the corresponding bound. We found the upper bounds for l_0 to be 15.7 fm (from comparison of the fine-structure improved Schrödinger description with the experiment), 0.136 fm (from comparison of the state-of-the-art theoretical value with the experiment), and 0.112 fm (from the experimental precision), respectively.

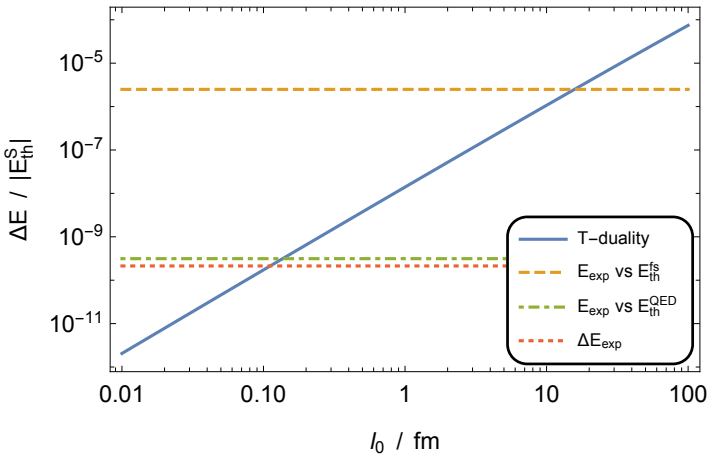

Figure 2. Normalized uncertainty in the hydrogen ground state energy. The possible T-duality contribution $\Delta E^{\mathrm{Td}}_{1,0}$ (solid, blue) increases with the zero-point length, l_0. The dashed (orange) and dot-dashed (green) lines show the differences between the experimental value on the one hand and the fine-structure corrected or the current theoretical value on the other hand—taking into account the respective standard deviations. The experimental error is presented by the dotted line (red).

3.2. Transition Frequency

Among all transitions of states in the hydrogen atom, the transition frequency between the $1S_{1/2}$ and the $2S_{1/2}$ level is experimentally known with the highest precision. The relative precision $\Delta\nu_{\mathrm{exp}}/\nu_{\mathrm{exp}}$ of the experimental value surpasses the relative precision of the absolute ground state energy, $\Delta E_{\mathrm{exp}}/E_{\mathrm{exp}}$, by five orders of magnitude. Therefore, we obtained more stringent upper bounds from the transition data than from the absolute energy data discussed above. The theoretical and experimental values of the transition frequencies associated with their uncertainties are presented in Table 2.

Table 2. Theoretical and experimental values of the $1S_{1/2} - 2S_{1/2}$ hydrogen transition frequency. The calculations of $\nu^{\mathrm{S}}_{\mathrm{th}}$ and $\nu^{\mathrm{fs}}_{\mathrm{th}}$ are based on the 2014 CODATA recommended values [19].

Frequency	Description	Value
$\nu^{\mathrm{S}}_{\mathrm{th}}$	Schrödinger	2 466 038 423(32) MHz
$\nu^{\mathrm{fs}}_{\mathrm{th}}$	Schrödinger, incl. fine-structure	2 466 068 517(32) MHz
$\nu^{\mathrm{QED}}_{\mathrm{th}}$	current theoretical value [29]	2 466 061 413.187 103(46) MHz
ν_{exp}	current experimental value [30]	2 466 061 413.187 018(11) MHz

Our approach is analogous to the case of the ground state energy. In Figure 3 one finds the l_0-dependent T-duality contribution to the transition frequency and the reference values.

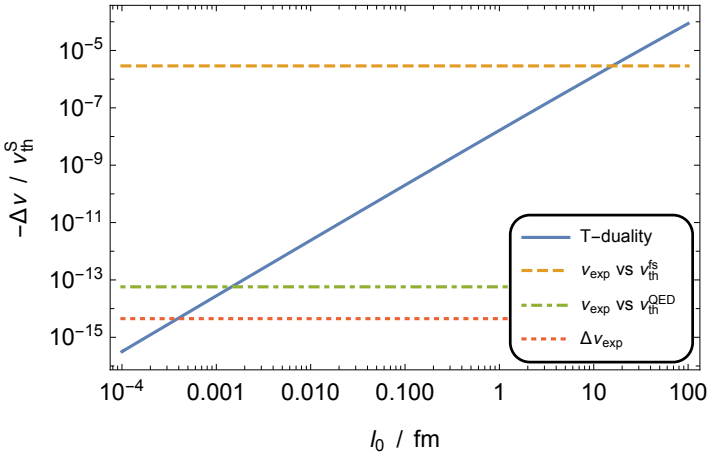

Figure 3. Normalized uncertainty in the $1S_{1/2} - 2S_{1/2}$ hydrogen transition frequency. The possible T-duality contribution $\Delta\nu^{Td}_{1S-2S}$ (solid, blue) increases with the zero-point length, l_0. The dashed (orange) line shows the difference between the experimental and the fine-structure corrected value. The dot-dashed (green) line shows the difference between the experimental and the current theoretical value. Both take into account the respective standard deviations. The experimental error is presented by the dotted line (red).

The corresponding upper bounds on l_0 are 15.7 fm (from comparison of the Schrödinger description including fine-structure corrections with the experiment), 1.45×10^{-3} fm (from comparison of the current theoretical value with the experiment), and 3.90×10^{-4} fm (from the experimental precision). For the sake of clarity and for contrasting with the other approach, the values are summarized in Table 3.

Table 3. Bounds of l_0. This table summarizes the findings from Section 3.

Reference Value	Upper Bound on l_0	Reference Value	Upper Bound on l_0
$E_{exp} - E_{th}^{fs}$	1.6×10^{-14} m	$\nu_{exp} - \nu_{th}^{fs}$	1.6×10^{-14} m
$E_{exp} - E_{th}^{QED}$	1.4×10^{-16} m	$\nu_{exp} - \nu_{th}^{QED}$	1.5×10^{-18} m
ΔE_{exp}	1.1×10^{-16} m	$\Delta\nu_{exp}$	3.9×10^{-19} m

4. Discussion

Below, we discuss the validity and self-consistency of the results of Section 2 first. Then, we comment on the bounds on the zero-point length.

One can classify the different contributions to the hydrogen energy levels in terms of powers of the fine-structure constant. Generally, the higher is the order of a term, the smaller is its absolute contribution. The Schrödinger value sets the scale at α^2 and the Schrödinger fine-structure correction occurs at α^4. The Dirac treatment reproduces the terms at order 4 and yields additional terms at order 6 and above. According to the standard theoretical description, further corrections set in at α^5 [19].

As presented in Equations (19) and (25), we obtained the corrections induced by the T-duality propagator in terms of Bessel and Struve functions. When expanding these results in powers of the fine-structure constant, Equations (21) and (27), we found the first manifestations at order α^4 and $\alpha^4 \ln(1/\alpha)$. At second order in perturbation theory, we expect terms starting with α^5. Similarly, mutual interactions with the fine-structure corrections can only appear at order 5 and above. Therefore, we ensure describing a proper observable since we have taken all contributions to order 4 into consideration.

The other parameter which determines the amplitude of the T-duality induced correction is the zero-point length. For small l_0, we found an approximately quadratic dependency, as evident in the

series expansions Equations (20) and (26). Furthermore, the logarithmic term is dominating and is responsible for the overall sign of the corrections. Both these features are evident in Figures 2 and 3.

We stress that the fine-structure corrected Schrödinger value for the ground state energy lies below the experimental one. Additionally, the current theoretical value hints at stronger binding than the current experimental one (cf. Table 1). Similarly, the analogous theoretical transition frequencies are found above the experimental counterpart (cf. Table 2). Thus, at qualitative level, a shift towards weaker binding energy and smaller transition frequency improves the match between the theoretical and experimental results. Indeed, both hold true for the T-duality corrections.

At a quantitative level, there are two ways of comparing potential theoretical contributions with experimental data. One can compare the conventional theoretical value with the experimentally measured one. Under the assumption that the discrepancy is generated by the novel effect only, one can derive a bound on the underlying parameter. Alternatively, one can focus on uncertainties and require the extra contribution to be smaller than the experimental accuracy. Then, the experimental standard deviation is regarded as the reference scale. The latter approach usually results in stronger constraints and is used commonly in literature, e.g., [20,22]. We followed both approaches. However, we refined the first way in a conservative manner: we did not just take into account the discrepancy between the theoretical and experimental value; we also took into consideration the respective standard deviations. That way, we obtained a less strict, but more reliable bound.

In this paper we address the ground state energy and the energy difference between the $1S_{1/2}$ and $2S_{1/2}$ levels. The latter observable turns out most suitable: Firstly, the corresponding transition frequency is known to a better precision, experimentally and theoretically. For instance, the experimental relative error exceeds the one of the ground state energy by five orders of magnitude. Indeed, this transition frequency is the most accurately known hydrogen spectral line [25]. Secondly, the difference between two levels is relative by definition: It is insensitive to global energy shifts.

Overall, we found constraints in the range 1.6×10^{-14} m down to 3.9×10^{-19} m. Table 3 shows a compilation of the bounds obtained. Limits in the range of 10^{-17} m were also found in related minimal length considerations [20,23] even though they arose from a different context: they rely on a generalization of the Heisenberg uncertainty relation while the limits presented here are the direct consequence of the T-duality propagator. There is a further sense of complementarity: they focus on a modification of the electron evolution and alter the Schrödinger or Dirac equation. In contrast, we applied the modified massless propagator to the electromagnetic field and studied the modified Coulomb potential while keeping the ordinary Schrödinger description. Although in both ways the energy contributions set in at α^4, we found an additional logarithmic contribution.

More precise experimental and theoretical results would be helpful to further restrict the size of minimal lengths and to explore the viable range of quantum gravity modifications. Based on a consistency condition for the smallest sensible size of black holes, the authors of [7] expected the value of the zero-point length at $l_0 = (2/3)^{3/4}\, l_\mathrm{P} \approx 0.8\, l_\mathrm{P}$, where l_P is the Planck length. Testing this length scale with the hydrogen atom would correspond to a relative precision of 10^{-47} for the ground state as well as for the transition frequency. While this seems out of reach with the techniques present today, astrophysical observations, e.g., of the maximum temperature of microscopic black holes, could provide stronger constraints and further insights.

5. Summary

String theory is a high-energy completion of quantum field theory and gravitation. Regarding quantum field excitations as strings instead of point-like particles, the authors of [4] derived the modified 4-dimensional propagator. It introduces a parameter called zero-point length, l_0, which is closely related to the self-dual radius of T-duality. This approach was applied to the context of black holes; differences to the general relativistic counterparts were identified [7].

In this paper, we investigated how the modified propagator manifests itself in the hydrogen atom. The hydrogen atom is a well suited system since it has been investigated to high precision

in theory and experiment. We derived the corrections to the hydrogen ground state energy and the $1S_{1/2} - 2S_{1/2}$ transition frequency by first order Rayleigh–Schrödinger perturbation theory. By comparison with experimental data, we could derive constraints on the zero-point length ranging down to $l_0 < 3.9 \times 10^{-19}$ m.

Author Contributions: Conceptualization, M.F.W. and M.B.; formal analysis, M.F.W.; funding acquisition, M.B.; investigation, M.F.W.; methodology, M.F.W.; project administration, M.F.W.; supervision, M.B.; validation, M.F.W.; visualization, M.F.W.; writing—original draft, M.F.W.; writing—review and editing, M.F.W. and M.B.

Funding: M.F.W. gratefully acknowledges the support by the Stiftung Polytechnische Gesellschaft Frankfurt am Main. This research was supported in part by the Helmholtz International Center for FAIR within the framework of the LOEWE program (Landesoffensive zur Entwicklung Wissenschaftlich-Ökonomischer Exzellenz) launched by the State of Hesse.

Conflicts of Interest: The authors declare no conflict of interest.

Appendix A. Useful Identities

The energy shifts from the T-duality contribution presented in Section 2.2 stem from non-standard integrals which result in special functions. The generalized form of these integrals results in

$$\int_0^\infty x^{2\nu-1}\left(u^2+x^2\right)^{\rho-1} \mathrm{e}^{-\mu x}\,\mathrm{d}x = \frac{u^{2\nu+2\rho-2}}{2\sqrt{\pi}\Gamma(1-\rho)}\, G_{1,3}^{3,1}\left(\mu^2u^2/4\,\middle|\,{}^{1-\nu}_{1-\rho-\nu,0,1/2}\right) \tag{A1}$$

for $|\arg u| < \pi/2$, $\Re\mu > 0$, and $\Re\nu > 0$ ([31] p. 351, Equation (3.389.2)). Here, $G_{p,q}^{m,n}\left(x\,\middle|\,{}^{a_1,\ldots,a_p}_{b_1,\ldots,b_q}\right)$ is the Meijer's G-function.

The resulting expressions can be simplified by using representations of the special functions in terms of the Meijer's G-function. In particular, the Bessel functions of the second kind, $Y_\nu(x)$, and the Struve functions, $\mathbf{H}_\nu(x)$, turn out useful ([31] p. 1034, Equation (9.34.2) and [31] p. 1035, Equation (9.34.5)):

$$Y_\nu(x)\,x^\alpha = 2^\alpha\, G_{1,3}^{2,0}\left(x^2/4\,\middle|\,{}^{(\alpha-\nu-1)/2}_{(\alpha-\nu)/2,(\alpha+\nu)/2,(\alpha-\nu-1)/2}\right) \tag{A2}$$

$$\mathbf{H}_\nu(x)\,x^\alpha = 2^\alpha\, G_{1,3}^{1,1}\left(x^2/4\,\middle|\,{}^{(\alpha+\nu+1)/2}_{(\alpha+\nu+1)/2,(\alpha-\nu)/2,(\alpha+\nu)/2}\right) \tag{A3}$$

References

1. Weinberg, S. *The Quantum Theory of Fields*; Volume II. Modern Applications; Cambridge University Press: Cambridge, UK, 2015; pp. 305–318.
2. De Rham, C. Massive Gravity. *Living Rev. Rel.* **2014**, *17*, 7. [CrossRef] [PubMed]
3. Maggiore, M. *Gravitational Waves*; Volume 1. Theory and Experiments; Oxford University Press: Oxford, UK, 2017; pp. 7–12, 70–74.
4. Fontanini, M.; Spallucci, E.; Padmanabhan, T. Zero-point length from string fluctuations. *Phys. Lett. B* **2006**, *633*, 627–630. [CrossRef]
5. Smailagic, A.; Spallucci, E.; Padmanabhan, T. String theory T duality and the zero point length of space-time. *arXiv* **2003**, arXiv:hep-th/0308122.
6. Spallucci, E.; Fontanini, M. Zero-point length, extra-dimensions and string T-duality. In *New Developments in String Theory Research*; Grece, S.A., Ed.; Nova Science Publishers, Inc.: Hauppauge, NY, USA, 2006; pp. 245–270.
7. Nicolini, P.; Spallucci, E.; Wondrak, M.F. Quantum Corrected Black Holes from String T-Duality. *Phys. Lett. B* **2019**, *797*, 134888. [CrossRef]
8. Padmanabhan, T. Duality and Zero-Point Length of Spacetime. *Phys. Rev. Lett.* **1997**, *78*, 1854–1857. [CrossRef]
9. Padmanabhan, T. Hypothesis of path integral duality. I. Quantum gravitational corrections to the propagator. *Phys. Rev. D* **1998**, *57*, 6206–6215. [CrossRef]
10. Srinivasan, K.; Sriramkumar, L.; Padmanabhan, T. The Hypothesis of path integral duality. II: Corrections to quantum field theoretic results. *Phys. Rev. D* **1998**, *58*, 044009. [CrossRef]

11. Sriramkumar, L.; Shankaranarayanan, S. Path integral duality and Planck scale corrections to the primordial spectrum in exponential inflation. *J. High Energy Phys.* **2006**, *12*, 050. [CrossRef]
12. Kothawala, D.; Sriramkumar, L.; Shankaranarayanan, S.; Padmanabhan, T. Path integral duality modified propagators in spacetimes with constant curvature. *Phys. Rev. D* **2009**, *80*, 044005. [CrossRef]
13. Kothawala, D.; Shankaranarayanan, S.; Sriramkumar, L. Quantum gravitational corrections to the stress-energy tensor around the BTZ black hole. *J. High Energy Phys.* **2008**, *09*, 095. [CrossRef]
14. Padmanabhan, T. A Measure for Quantum Paths, Gravity and Spacetime Microstructure *arXiv* **2019**, arXiv:gr-qc/1908.10872.
15. Shankaranarayanan, S.; Padmanabhan, T. Hypothesis of path integral duality: Applications to QED. *Int. J. Mod. Phys. D* **2001**, *10*, 351–366. [CrossRef]
16. Ohanian, H.C. Finite quantum electrodynamics with a gravitationally smeared propagator. *Phys. Rev. D* **1997**, *55*, 5140–5146. [CrossRef]
17. Ohanian, H.C. Finite quantum electrodynamics and gauge invariance. *Nuovo Cim. A* **1997**, *110*, 751–756.
18. Ohanian, H.C. Smearing of propagators by gravitational fluctuations on the Planck scale. *Phys. Rev. D* **1999**, *60*, 104051. [CrossRef]
19. Mohr, P.J.; Newell, D.B.; Taylor, B.N. CODATA Recommended Values of the Fundamental Physical Constants: 2014. *Rev. Mod. Phys.* **2016**, *88*, 035009. [CrossRef]
20. Brau, F. Minimal length uncertainty relation and hydrogen atom. *J. Phys. A* **1999**, *32*, 7691–7696. [CrossRef]
21. Akhoury, R.; Yao, Y.P. Minimal length uncertainty relation and the hydrogen spectrum. *Phys. Lett. B* **2003**, *572*, 37–42. [CrossRef]
22. Hossenfelder, S.; Bleicher, M.; Hofmann, S.; Ruppert, J.; Scherer, S.; Stöcker, H. Signatures in the Planck regime. *Phys. Lett. B* **2003**, *575*, 85–99. [CrossRef]
23. Antonacci Oakes, T.L.; Francisco, R.O.; Fabris, J.C.; Nogueira, J.A. Ground State of the Hydrogen Atom via Dirac Equation in a Minimal Length Scenario. *Eur. Phys. J. C* **2013**, *73*, 2495. [CrossRef]
24. Wondrak, M.F.; Nicolini, P.; Bleicher, M. Unparticle contribution to the hydrogen atom ground state energy. *Phys. Lett. B* **2016**, *759*, 589–592. [CrossRef]
25. Kramida, A.E. A critical compilation of experimental data on spectral lines and energy levels of hydrogen, deuterium, and tritium. *Atom. Data Nucl. Data Tables* **2010**, *96*, 586–644; Erratum in **2019**, *126*, 295. [CrossRef]
26. Greiner, W. *Quantenmechanik. Einführung*; Wissenschaftlicher Verlag Harri Deutsch: Frankfurt am Main, Germany, 2005; pp. 219–234.
27. Schwabl, F. *Quantenmechanik (QM I); Eine Einführung*; Springer: Berlin, Germany, 2007; pp. 121–142, 217–227.
28. Blumenhagen, R.; Cvetic, M.; Langacker, P.; Shiu, G. Toward realistic intersecting D-brane models. *Annu. Rev. Nucl. Part. Sci.* **2005**, *55*, 71–139. [CrossRef]
29. Jentschura, U.D.; Kotochigova, S.; LeBigot, E.O.; Mohr, P.J.; Taylor, B.N. *The Energy Levels of Hydrogen and Deuterium (Version 2.1)*; National Institute of Standards and Technology: Gaithersburg, MD, USA, 2005. Available online: http://physics.nist.gov/HDEL (accessed on 30 August 2019).
30. Matveev, A.; Parthey, C.G.; Predehl, K.; Alnis, J.; Beyer, A.; Holzwarth, R.; Udem, T.; Wilken, T.; Kolachevsky, N.; Abgrall, M.; et al. Precision Measurement of the Hydrogen 1S-2S Frequency via a 920-km Fiber Link. *Phys. Rev. Lett.* **2013**, *110*, 230801. [CrossRef]
31. Gradshteyn, I.S.; Ryzhik, I.M. *Tables of Integrals, Series, and Products*, 7th ed.; Elsevier Academic Press: London, UK, 2007.